J. Fluid Mech. (1992), *vol.* 245, *pp.* 249–261

On the evolution of roll waves

By C. KRANENBURG

Department of Civil Engineering, Delft University of Technology, PO Box 5048, 2600 GA Delft, The Netherlands

(Received 11 November 1991 and in revised form 4 June 1992)

An amplitude evolution equation is derived for roll waves that occur in a uniform open-channel flow down an incline. A periodic series of roll waves, which is a manifestation of the instability of high-velocity turbulent flow, is shown to be itself unstable to subharmonic disturbances. These disturbances develop into longer and higher roll waves. In this way roll waves tend to increase in size as time goes on, in agreement with experimental evidence.

1. Introduction

The turbulent flow of a sheet of water down an open inclined channel may become unstable when the Froude number exceeds a critical value. The instability arises when the kinematic-wave velocity of the friction-dominated flow becomes greater than the propagation velocity of shallow-water waves, which is the largest propagation velocity of continuous waves in a flow of this type (e.g. Whitham 1974, pp. 75, 85). As a consequence, the unstable uniform flow breaks down in a series of breaking waves or bores that are separated by sections of gradually varying flow. In favourable circumstances these waves are more or less periodic, and then are known as roll waves. These waves occur easily in certain man-made conduits, such as run-off channels.

The mechanism leading to the instability was revealed by Jeffreys (1925) in an early study of roll waves. Photographs illustrating the periodic nature of roll waves have been published by Cornish (1934). Dressler (1949) used the shallow-water equations augmented by a term accounting for the turbulent bottom friction to construct nonlinear periodic solutions that consist of piecewise smooth profiles separated by discontinuities representing the bores. Novik (1971) proposed a 'model equation', the Burgers equation, to which a linear amplification term was added, and obtained continuous periodic solutions of roll wave type. Following Whitham (1974, p. 482), Needham & Merkin (1984) further extended the shallow-water equations by adding a diffusive term to the momentum equation and were also able to show that continuous roll-wave solutions exist when the uniform flow is unstable.

In all this theoretical work the analyses have been restricted to periodic roll waves. However, experimental evidence indicates that roll waves are quasi-periodic at best. Faster bores tend to overtake slower ones and subsequently combine to form longer and higher roll waves. Such behaviour was observed in the laboratory by, among others, Mayer (1961) for open-channel flow and Alavian (1986) for two-layer underflow down an incline.

In this paper I derive an amplitude evolution equation for small (but finite) amplitude roll waves starting from equations similar to those used by Needham & Merkin (1984), and thus recover Novik's (1971) equation. It is shown, through numerical integration of the evolution equation, that periodic roll waves are unstable to a subharmonic disturbance. While growing, such a disturbance annihilates these roll waves within a finite time interval through the mechanism of shock coalescence, and develops into roll waves of larger size. The method of deriving the evolution equation was also used in a stability analysis of non-uniform flow (Kranenburg 1990).

2. Amplitude evolution equation for weakly nonlinear waves

2.1. *Equations of motion*

The proper model description of bores is different for breaking and non-breaking bores. In both cases hydrodynamical energy is removed from the bore (Benjamin & Lighthill 1954). In non-breaking bores the energy is radiated in the downstream direction in the form of waves, which are attended by a non-hydrostatic pressure distribution. Such waves, and the related deviations from the quasi-hydrostatic pressure distribution, are not present with a breaking bore. In this case hydrodynamical energy is dissipated by turbulence produced in the bore. To describe roll waves we therefore assume a quasi-hydrostatic pressure distribution.

We further assume that the slope of the channel is constant, and that the channel is wide so that sidewall friction may be neglected. The shallow-water equations of continuity and momentum then are (e.g. Liggett 1975, §§2.2, 2.5)

$$\frac{\partial h}{\partial t}+\frac{\partial}{\partial x}(\bar{u}h) = 0, \tag{2.1}$$

$$\frac{\partial}{\partial t}(\bar{u}h)+\frac{\partial}{\partial x}\int_0^h u^2(x,z,t)\,\mathrm{d}z+g'h\frac{\partial h}{\partial x} \approx g'hS-\frac{\tau_\mathrm{b}}{\rho}, \tag{2.2}$$

where (see figure 1) x is the coordinate along the bottom of the channel, z the coordinate perpendicular to it (z is positive in the upward direction), u the velocity component (averaged to eliminate turbulent fluctuations) in the x-direction, $\bar{u}$ its depth-averaged value, h the water depth measured in the z-direction, t time, τ_b the bed friction, ρ the density of water, $S = \tan\phi$ the slope of the channel, and $g' = g\cos\phi$. Here ϕ is the angle of inclination of the channel to the horizontal, and g is the acceleration due to gravity.

The bed friction is modelled assuming quasi-steady and quasi-uniform flow. We use the Chézy formula for turbulent flow known from the hydraulics literature,

$$\frac{\tau_\mathrm{b}}{\rho} = C_\mathrm{f}\,\bar{u}^2, \tag{2.3}$$

where C_f is an empirical friction coefficient depending on the Reynolds number and the relative roughness height of the bed. At large Reynolds numbers C_f depends mainly on the latter parameter, and then is about 0.002–0.006 for relatively smooth to moderately rough channel bottoms. Variations in the coefficient C_f influence the stability boundary (Liggett 1975, §6.2), but in a more qualitative sense do not essentially affect the results. For convenience we therefore assume C_f to be constant.

As a final step for arriving at a closed set of equations, the momentum transfer term in (2.2) must be modelled. The usual approach for gradually varying flow is to introduce a profile coefficient $\alpha(\alpha > 1)$ so that

$$\int_0^h u^2\,\mathrm{d}z \approx \alpha\bar{u}^2h,$$

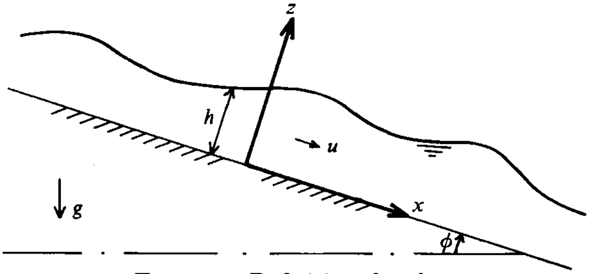

FIGURE 1. Definition sketch.

assuming α is constant. However, in the case under consideration the profile coefficient is certainly not constant. In the bores a surface roller occurs, and the recirculating flow results in velocity profiles that are very non-uniform. Since in the bores the velocity gradient $\partial\bar{u}/\partial x$ is always negative while its absolute value is large, we relate the momentum transfer term to this velocity gradient. A simple model is

$$\int_0^h u^2\,\mathrm{d}z \approx \alpha\bar{u}^2 h - \nu h\frac{\partial\bar{u}}{\partial x}, \tag{2.4}$$

where α is a constant again, and ν is an empirical coefficient ($\nu > 0$) with the dimensions of a kinematic viscosity. The comment made on variations in C_f also applies to values of α differing from one: this coefficient influences the quantitative results, but the general behaviour of solutions is not changed. We therefore consider the case $\alpha = 1$ only.

After substitution from (2.1), (2.3) and (2.4), the momentum equation (2.2) can then be written as

$$\frac{\partial\bar{u}}{\partial t}+\bar{u}\frac{\partial\bar{u}}{\partial x}+g'\frac{\partial h}{\partial x} = g'S - C_f\frac{\bar{u}^2}{h}+\frac{1}{h}\frac{\partial}{\partial x}\left(h\nu\frac{\partial\bar{u}}{\partial x}\right). \tag{2.5}$$

The solution of the equations of motion, (2.1) and (2.5), for the undisturbed uniform flow, in which the velocity $\bar{u}_0$ and water depth h_0 are constant, is

$$\bar{u}_0^2 = \frac{g'Sh_0}{C_f}. \tag{2.6}$$

A linear stability analysis of (2.1) and (2.5) yields as a necessary and sufficient condition for the uniform flow to be stable the well-known result

$$F \leqslant 2, \tag{2.7}$$

where F is the Froude number defined by $F^2 = \bar{u}_0^2/(g'h_0)$. Different critical Froude numbers are obtained for friction laws that differ from (2.3) and for a profile coefficient α greater than one. Needham & Merkin (1984) and Merkin & Needham (1986) showed rigorously that steady, periodic solutions of (2.1) and (2.5) will exist if $F > 2$.

Dimensionless variables are introduced according to

$$h = h_0\tilde{h}, \quad \bar{u} = (g'h_0)^{\frac{1}{2}}\tilde{u}, \quad x = h_0\tilde{x}, \quad t = (h_0/g')^{\frac{1}{2}}\tilde{t}, \quad \nu h = \nu_0 h_0\tilde{Q},$$

where a tilde denotes a dimensionless variable and ν_0 is a constant, the value of which is to be chosen later. Together with (2.6), equations (2.1) and (2.5) become in dimensionless form (the tildes are dropped)

$$\frac{\partial h}{\partial t}+\frac{\partial}{\partial x}(uh)=0, \tag{2.8}$$

$$\frac{\partial u}{\partial t}+u\frac{\partial u}{\partial x}+\frac{\partial h}{\partial x}=S-C_f\frac{u^2}{h}+\frac{1}{Rh}\frac{\partial}{\partial x}\left(Q\frac{\partial u}{\partial x}\right), \tag{2.9}$$

where R is a Reynolds number defined by $R=(g'h_0)^{\frac{1}{2}}h_0/\nu_0$.

2.2. *Asymptotic expansion*

Slowly deforming, weakly nonlinear waves superimposed on the basic uniform flow can be described by the scalings (e.g. Craik 1985, p. 173, where further references are given)

$$h=1+\epsilon A(\xi,\tau) \quad u=F+\epsilon U(\xi,\tau), \tag{2.10}$$

where

$$\xi=\epsilon(x-ct) \quad \tau=\epsilon^2 t. \tag{2.11}$$

Here ξ and τ are transformed coordinate and time, c is the long-wave speed in the undisturbed flow, and ϵ a small parameter that is to be related to the friction coefficient C_f. On substitution the equations of motion become

$$\frac{\partial}{\partial \xi}[(F-c)A+U]+\epsilon\left[\frac{\partial A}{\partial \tau}+\frac{\partial}{\partial \xi}(AU)\right]=0, \tag{2.12}$$

$$\frac{\partial}{\partial \xi}[A+(F-c)U]+\epsilon\left[\frac{\partial U}{\partial \tau}+U\frac{\partial U}{\partial \xi}+\frac{C_f}{\epsilon^2}F(2U-FA)\right.$$
$$\left.+\frac{C_f}{\epsilon}(U-FA)^2-\frac{1}{R(1+\epsilon A)}\frac{\partial}{\partial \xi}\left(Q\frac{\partial U}{\partial \xi}\right)\right]=O(\epsilon C_f). \tag{2.13}$$

Restricting the analysis to small flow resistance ($C_f \ll 1$), we choose the parameter ϵ such that bottom friction does not enter the analysis before the second-order approximation. This is achieved by setting $\epsilon^2=C_f$. Since the Froude number is of order one, it follows from (2.6) that the assumption of small flow resistance implies a small slope ($S \ll 1$). Proper treatment of the bores requires the convective and diffusive terms to be of the same order of magnitude. We therefore take $R=1$, which determines the constant ν_0.

To first order, (2.12) and (2.13) give the long-wave velocities for the undisturbed flow,

$$c=F\pm 1,$$

and leading terms of the Riemann invariants

$$U=\pm A+O(\epsilon).$$

Since instabilities and roll waves travel in the downstream direction, we consider the case $c=F+1$, $U=A+O(\epsilon)$ only. As a second-order approximation we put

$$U=A+\epsilon\left(pA^2+qV+rQ\frac{\partial A}{\partial \xi}\right)+O(\epsilon^2), \tag{2.14}$$

where V is a function of ξ and τ given by $\partial V/\partial \xi=A$, and p, q and r are constants. Substituting from (2.14), equations (2.12) and (2.13) give

$$p=-\tfrac{1}{4}, \quad q=\tfrac{1}{2}F(2-F), \quad r=-\tfrac{1}{2}.$$

Eliminating the first-order terms between (2.12) and (2.13) by adding these equations yields another second-order equation for A and U,

$$\frac{\partial A}{\partial \tau}+\frac{\partial U}{\partial \tau}+\frac{\partial}{\partial \xi}(AU+\tfrac{1}{2}U^2)+F(2U-FA)=\frac{\partial}{\partial \xi}\left(Q\frac{\partial U}{\partial \xi}\right)+O(\epsilon). \tag{2.15}$$

To second order the amplitude evolution equation as given by (2.14) and (2.15) is

$$2\frac{\partial A}{\partial \tau}+3A\frac{\partial A}{\partial \xi}=F(F-2)A+\frac{\partial}{\partial \xi}\left(Q\frac{\partial A}{\partial \xi}\right). \tag{2.16}$$

This equation is a modified Burgers equation that is known from other applications, including the nonlinear propagation of sound in an exponential channel (Crighton 1979). Novik (1971) postulated (2.16) as a model equation describing roll waves, without, however, giving a derivation. A linearizing transformation for this equation is not known (Kaup 1980; Nimmo & Crighton 1982).

Away from possible bores the diffusive term in (2.16) is negligible. Integrating the reduced equation along characteristic curves shows that a long-wave disturbance will grow, and hence the uniform flow will be unstable, if (2.7) is violated. In the remaining part of this paper only the unstable flow for which $F>2$ is analysed. As opposed to the Burgers equation, equation (2.16) allows steady, periodic solutions if $F>2$ and Q does not depend explicitly on ξ (Novik 1971).

The function $V=\int A\,\mathrm{d}\xi$ occurring in (2.14) must remain bounded to evade secular behaviour of solutions to (2.16). Such behaviour would result in non-uniformity of the approximation for large times, which in itself is not illogical when dealing with unstable solutions. However, for the asymptotic expansion to be of some value, solutions should be uniformly bounded. Restricting the analysis to initial-value problems, the function V remains bounded provided the spatially averaged value of the amplitude A vanishes in any domain of length $O(1)$. In particular, for spatially periodic solutions it must be required that, to second order,

$$\int_L A(\xi,\tau)\,\mathrm{d}\xi=0 \quad (\tau \geqslant 0), \tag{2.17}$$

where L is a wavelength of order one. On inspection of (2.16) it follows that if the integral in (2.17) is zero at $\tau=0$, it will be zero for all $\tau>0$.

Rescaling of the variables according to

$$A=\frac{F(F-2)}{3l}\eta,\quad Q=\frac{F(F-2)}{l^2}\delta,\quad \xi=lx^*,\quad \tau=\frac{2}{F(F-2)}t^*,$$

where l is a lengthscale, changes (2.16) to the standard form (the asterisks are dropped)

$$\frac{\partial \eta}{\partial t}+\eta\frac{\partial \eta}{\partial x}=\eta+\frac{\partial}{\partial x}\left(\delta\frac{\partial \eta}{\partial x}\right). \tag{2.18}$$

3. Propagation of bores

In this section we consider in some detail the propagation of bores (referred to as shock waves hereinafter) to illustrate some properties of solutions of (2.18), and to make a comparison between numerical and analytical solutions. The analysis is along the lines indicated by Whitham (1974, pp. 30, 61).

A shock condition can be derived by integrating (2.18) on a narrow domain containing the shock wave and neglecting higher-order contributions. This gives for the propagation velocity c_s of the shock wave

$$c_s = \tfrac{1}{2}(\eta_1+\eta_2), \tag{3.1}$$

where η_1 and η_2 are the water-level elevations just ahead ($x = x_s^+$) and behind ($x = x_s^-$) the shock wave.

The propagation of a shock wave can be calculated analytically, in an approximate way, by fitting (3.1) to continuous solutions of (2.18) in which δ is set equal to zero thus reducing it to a kinematic-wave equation. The characteristic curves of the reduced equation are given by

$$\mathrm{d}t = \frac{\mathrm{d}x}{\eta} = \frac{\mathrm{d}\eta}{\eta}. \tag{3.2}$$

The solution of (3.2) is

$$\eta = f(\zeta)\,\mathrm{e}^t, \quad x = \zeta + f(\zeta)\,(\mathrm{e}^t - 1), \tag{3.3a, b}$$

where $f(\zeta) = \eta(\zeta, 0)$ represents the initial condition.

A shock wave forms when $\partial x/\partial\zeta = 0$. Equation (3.3$b$) then gives the instant, $t = t_s$, at which a shock wave arises on the characteristic curve starting at $x = \zeta$ as

$$t_s = \ln\left(1 - \frac{1}{\mathrm{d}f/\mathrm{d}\zeta}\right). \tag{3.4}$$

Apparently a shock will develop only if $\mathrm{d}f/\mathrm{d}\zeta < 0$. According to (3.3$a$), η is proportional to f so that a necessary condition for shock stability is $\eta_2 > \eta_1$.

Equation (3.1) implies that shock waves of different mean heights travel at different speeds. When several shock waves are present, one shock wave sooner or later overtakes another. After confluence of two shock waves they coalesce and continue to propagate as a single shock wave.

To illustrate the argument outlined, and to verify the numerical method used to solve (2.18), we consider two examples in which coalescence of shock waves occurs. The first example is deliberately chosen so as to demonstrate non-uniform behaviour for large times. The initial condition is

$$\eta(x,0) = \begin{cases} ax & (|x| < s_1), \\ bx & (s_1 < |x| < s_2), \\ 0 & (s_2 < |x|), \end{cases} \tag{3.5}$$

where s_1, s_2, a and b are constants, and $0 < b < a < 1$. Shocks are initially present at $x = \pm s_1$ and $x = \pm s_2$. The average value of the initial wave elevations vanishes, as required. We consider only the domain $x \geqslant 0$ because of symmetry.

The continuous solutions (3.3) become

$$\eta(x,t) = \begin{cases} \dfrac{ax\,\mathrm{e}^t}{1-a+a\,\mathrm{e}^t} & (0 \leqslant x < x_1), \quad (3.6a) \\[2ex] \dfrac{bx\,\mathrm{e}^t}{1-b+b\,\mathrm{e}^t} & (x_1 < x < x_2), \quad (3.6b) \end{cases}$$

where $x = x_1$ and $x = x_2$ are the positions of the shocks initially at $x = s_1$ and $x = s_2$.

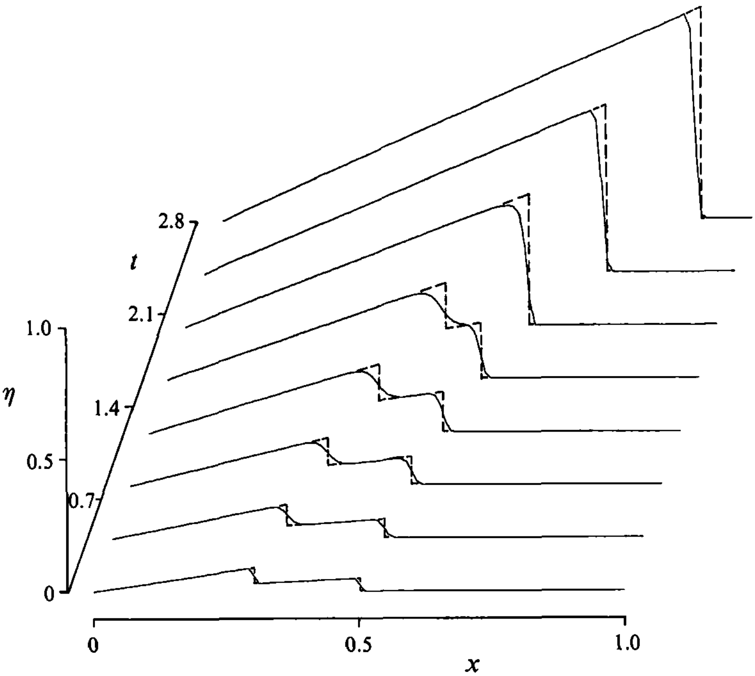

FIGURE 2. Example of shock-wave propagation and comparison with numerical results. Only results for $x \geqslant 0$ are shown because of symmetry; -----, analytical results, ———, numerical results ($\delta_0 = 1.2\times 10^{-4}$, $\beta_1 = 0.4$, $\beta_2 = 0.5$).

Substituting from (3.1) and (3.6), using the relation $c_s = \mathrm{d}x/\mathrm{d}t$ and integrating give these positions as

$$x_1 = s_1[(1-a+a\,\mathrm{e}^t)(1-b+b\,\mathrm{e}^t)]^{\frac{1}{2}},$$
$$x_2 = s_2(1-\beta+\beta\,\mathrm{e}^t)^{\frac{1}{2}}.$$

The shocks combine when $x_1 = x_2(=x_c)$. The coordinate x_c and time $(t = t_c)$ of confluence are

$$x_c = s_2\left[1+\frac{b}{a}\left(\frac{s_2^2}{s_1^2}-1\right)\right]^{\frac{1}{2}},\quad t_c = \ln\left[1+\frac{1}{a}\left(\frac{s_2^2}{s_1^2}-1\right)\right].$$

The continuous solution for $t > t_c$ is given by (3.6*a*). The position, $x = x_s$, of the single shock remaining is given by

$$x_s = x_c\left(\frac{1-a+a\,\mathrm{e}^t}{1-a+a\,\mathrm{e}^{t_c}}\right)^{\frac{1}{2}}\quad (t \geqslant t_c).$$

These solutions are shown in figure 2 for $a = 0.3$, $b = 0.1$, $s_1 = 0.3$, $s_2 = 0.5$. As time goes on, the remaining shock wave continues to propagate in the positive x-direction while according to (3.6*a*) $\eta \to x$ as $t \to \infty$. Although the mean value of η is always zero (the negative x-axis is now included again), the smallest domain in which this is true grows without bound and consequently the approximation is non-uniform.

The numerical calculation of shock waves requires non-zero (positive) values of the viscosity δ, not only for the solutions to become continuous, but also to suppress certain oscillations produced by the finite-difference scheme used. Details of the numerical method applied are presented in the Appendix. The numerical results shown in figure 2 are seen to agree well with the analytical solution.

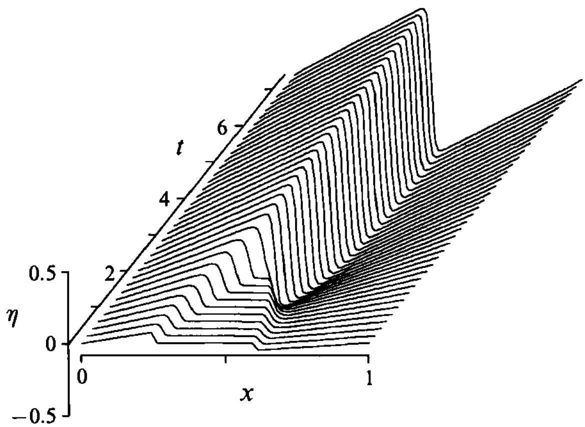

FIGURE 3. Example of stable position of shock wave as $t \to \infty$ (numerical results, $\delta_0 = 0.9 \times 10^{-4}$, $\beta_1 = 0.9$, $\beta_2 = 0.7$).

The initial condition and boundary conditions of the second example are such that the approximation is uniform. It is given by

$$\eta(x,0) = \begin{cases} 0.32x & (0 < x < 0.25) \\ -0.125(1-x) & (0.6 < x < 1) \\ 0 & (0.25 < x < 0.6). \end{cases}$$

The boundary conditions are $\eta(0,t) = \eta(1,t) = 0$. Results of numerical calculations are shown in figure 3.

These examples indicate that the shock waves becoming stationary as $t \to \infty$ is a necessary condition for the approximation to be uniform. As will be seen in the next section, periodic solutions always satisfy this condition provided (2.17) holds good. This condition is not always sufficient, however. For example, the solution of the initial-value problem with $\eta(x,0) = -x\exp(-x^2/a^2)$ where $-\infty < x < \infty$ and $a^2 \ll 1$, or a similar initial form, yields a solitary shock wave that is stationary at $x = 0$. However, the height and the lengthscale of the wave system finally became proportional to $\delta_0^{\frac{1}{3}}t$, where δ_0 is the value of δ when $\eta = \partial\eta/\partial x = 0$ (see Appendix). The factor $\delta_0^{\frac{1}{3}}$ implies that in this case the non-uniformity of the approximation is caused by viscosity.

4. Instability of periodic solutions

In this section we show, through numerical computations, that the initial-value problem for periodic solutions of (2.18) is ill-posed and analyse the generic behaviour of such solutions in some detail. To this end we assume spatially periodic initial conditions satisfying (2.17) by putting

$$\eta(x,0) = \sum_k a_k \sin(2k\pi x + \psi_k), \tag{4.1}$$

where a_k is an amplitude, ψ_k a phase angle, and the summation is over a number of preselected values of the integer k ($k \geqslant 1$). The evolution of the amplitude η is computed in the domain $0 \leqslant x \leqslant 1$.

Figure 4 shows the development of a simple sine wave disturbance with $k = 4$ and

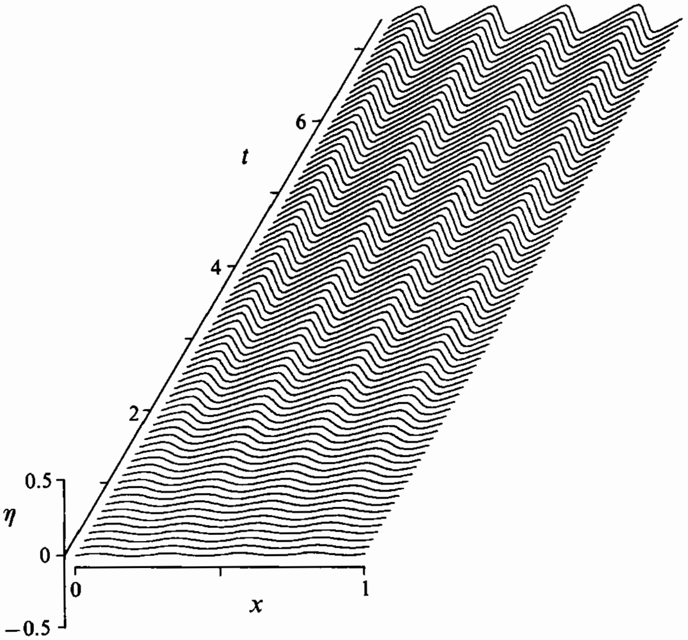

FIGURE 4. Evolution of a small-amplitude sine wave into a series of periodic roll waves ($\delta_0 = 4.2 \times 10^{-4}$, $\beta_1 = 1.4$, $\beta_2 = 0.6$).

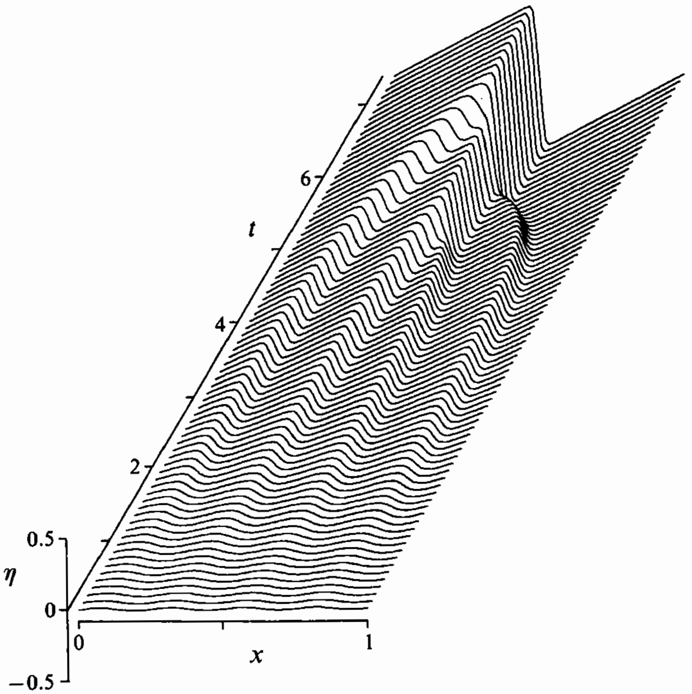

FIGURE 5. Coalescence of shock waves. Initial condition of figure 4 to which a subharmonic sine wave of smaller amplitude was added ($\delta_0 = 4.2 \times 10^{-4}$), $\beta_1 = 1.4$, $\beta_2 = 0.6$).

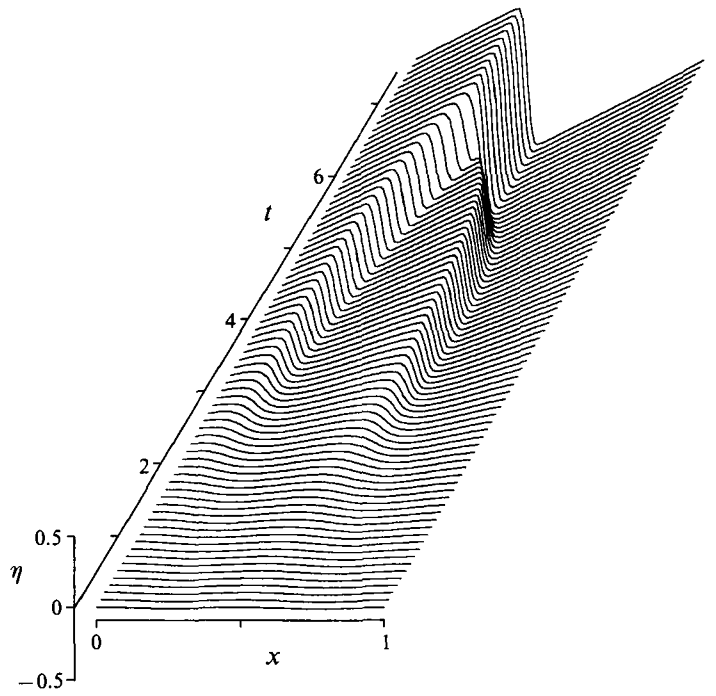

FIGURE 6. Phase shift of final roll waves caused by a higher-mode initial disturbance ($\delta_0 = 4.2 \times 10^{-4}$, $\beta_1 = 1.4$, $\beta_2 = 0.7$).

$(a_4, \psi_4) = (0.01, 0)$ into a periodic train of shock waves separating sections with gradually varying flow. The solution for time going to infinity is of the type considered by Dressler (1949), Novik (1971) and Needham & Merkin (1984). However, the solution will be completely different if a subharmonic disturbance is present. Figure 5 shows the results for the case where a sine wave with $k = 1$ and $(a_1, \psi_1) = (0.001, 0)$ is added to the previous initial condition. Initially a train of roll waves appears to develop as in figure 4, but gradually the influence of the subharmonic wave becomes noticeable: the shock waves are displaced from their equilibrium position so that their propagation velocities no longer vanish, see (3.1). The four shock waves present move towards the centre ($x = 0.5$) and coalesce at that location, first the two central shocks and then the two peripheral ones. After that steady roll waves of greater wavelength and wave height remain, as if the $k = 1$ wave only had been present as an initial condition. Reducing the initial amplitude of the subharmonic only delays the approach to the final steady solution.

In general, the higher wavenumber initial waves do influence the final result in that they generate a phase shift of the $k = 1$ wave. An example with $(a_1, \psi_1) = (0.001, 0)$ and $(a_2, \psi_2) = (0.005, \frac{1}{2}\pi)$ is shown in figure 6. The $k = 1$ wave gradually develops into a shock wave while travelling through the disturbances caused by the $k = 2$ wave, thus experiencing a phase shift from $\psi = 0$.

The results indicate that if a spectrum of wave components is initially present, all components will influence the solution during a transient period and jointly will produce a phase shift of the final steady solution due to the longest ($k = 1$) wave. Such behaviour is illustrated in figure 7 for a case where the initial amplitudes increase with k and the phase angles are chosen at random (except or $k = 1$), see table 1.

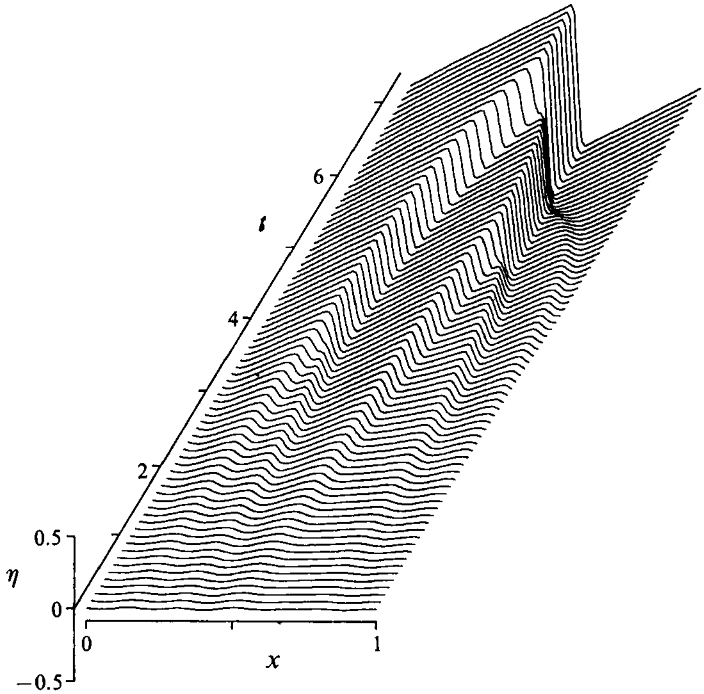

FIGURE 7. Evolution of roll waves from a spectrum of initial disturbances ($\delta_0 = 1.8\times10^{-4}$, $\beta_1 = 0.9$, $\beta_2 = 0.5$).

k	1	2	3	4	5	6
a_k	0.001	0.0015	0.002	0.0025	0.003	0.0035
ψ_k	0	6.16	4.90	1.21	4.01	2.46

TABLE 1. Initial conditions for results shown in figure 7

5. Conclusion

The calculations presented are restricted to small-amplitude waves, but nevertheless they show some unusual effects. The initial problem for the unstable situation is ill-posed: small-amplitude subharmonic disturbances eventually produce a completely different solution. Small initial perturbations grow and thus lead to disorder, but in the long run all waves but the longest are annihilated. The profile of the surviving wave is always the same, the shorter waves only causing a phase shift.

The theoretical results agree, at least in a qualitative sense, with the observed tendency of roll waves on an incline of sufficient length to rearrange and combine to form longer and higher waves (Mayer 1961; Alavian 1986). Quantitative comparison with experimental results is difficult because of the sensitivity to initial (or boundary) conditions noted.

Figures 5–7 appear to indicate that the process of wave growth comes to an end after some time. However, this is only because an upper bound to the wavelengths of the initial perturbations was assumed. In real flows such a cutoff in the spectrum of wavelengths will not exist so that the coalescence of bores continues to produce waves of increasing size. The asymptotic method used is not suitable for describing this continuing wave growth. Instead, the full equations of motion (2.8) and (2.9) would be needed.

Appendix. Finite-difference scheme

Equation (2.18) is cast in conservation form, $\partial\eta/\partial t+\partial G/\partial x = \eta$ where $G=\frac{1}{2}\eta^2-\delta\partial\eta/\partial x$. These equations are approximated by finite-difference equations according to

$$\frac{\eta_i^{n+1}-\eta_i^n}{\Delta t}+\frac{G_{i+1}^n-G_{i-1}^n}{\Delta x}=\frac{\eta_i^n+\eta_i^{n+1}}{2}, \tag{A 1}$$

$$G_{i+1}^n=\frac{1}{2}\left(\frac{\eta_i^n+\eta_{i+2}^n}{2}\right)^2-\delta_{i+1}^n\frac{\eta_{i+2}^n-\eta_i^n}{\Delta x}, \tag{A 2}$$

where Δx and Δt are space and time mesh sizes, and i and n denote mesh points on the x and time axes. The term $\partial G/\partial x$ is approximated by central differences. The time integration of this term is explicit, and that of the term on the right-hand side of (A 1) is implicit. The truncation error is $O(\Delta x^2, \Delta t)$.

In most cases the viscosity δ does not affect the overall results as long as it remains small outside the shock waves, and therefore is chosen so as to suppress numerically produced oscillations. The expression adopted is

$$\delta=\left[\delta_0^2+\left(\beta_1\,\Delta x^2\frac{\partial\eta}{\partial x}\right)^2+(\beta_2\,\Delta x\eta)^2\right]^{\frac{1}{2}}, \tag{A 3}$$

where δ_0, β_1 and β_2 are constants. The first term on the right-hand side of (A 3) represents a physical viscosity, whereas the second and third terms represent artificial contributions needed for numerical reasons. The second term smears a shock out so that its thickness is of the order Δx (Roache 1976, §VD), and the third eliminates numerical oscillations in regions where $|\partial\eta/\partial x|$ is small. The first term was found to aid the suppression of a wiggle at the upward zero-crossings. The computations shown were made for $\Delta x = \Delta t = 0.01$, while the coefficients in (A 3) were taken to be small so as to reduce the numerical damping in each case as much as possible.

REFERENCES

ALAVIAN, V. 1986 Behavior of density currents on an incline. *J. Hydraul. Engng ASCE* **112**, 27–42.

BENJAMIN, T. B. & LIGHTHILL, M. J. 1954 On cnoidal waves and bores. *Proc. R. Soc. Lond.* A**224**, 448–460.

CORNISH, V. 1934 *Ocean Waves and Kindred Geophysical Phenomena*. Cambridge University Press.

CRAIK, A. D. D. 1985 *Wave Interactions and Fluid Flows*. Cambridge University Press.

CRIGHTON, D. G. 1979 Model equations of nonlinear acoustics. *Ann. Rev. Fluid Mech.* **11**, 11–33.

DRESSLER, R. F. 1949 Mathematical solution of the problem of roll-waves in inclined open channels. *Commun. Pure Appl. Maths* **2**, 149–194.

JEFFREYS, H. 1925 The flow of water in an inclined channel of rectangular section. *Phil. Mag.* **49**, 793–807.

KAUP, D. J. 1980 The Estabrook–Wahlquist method with examples of application. *Physica* D**1**, 391–411.

KRANENBURG, C. 1990 On the stability of gradually varying flow in wide open channels. *J. Hydraul. Res.* **28**, 621–628.

LIGGETT, J. A. 1975 In *Unsteady Flow in Open Channels* (ed. K. Mahmood & V. Yevjevich), vol. 1. Water Resources Publications.

MAYER, P. G. 1961 Roll waves and slug flows in inclined open channels. *Trans. ASCE*, 505–535.

MERKIN, J. H. & NEEDHAM, D. J. 1986 An infinite period bifurcation arising in roll waves down an open inclined channel. *Proc. R. Soc. Lond.* A**405**, 103–116.

NEEDHAM, D. J. & MERKIN, J. H. 1984 On roll waves down an open inclined channel. *Proc. R. Soc. Lond.* A**394**, 259–278.

NIMMO, J. J. C. & CRIGHTON, D. G. 1982 Bäcklund transformations for nonlinear parabolic equations: the general results. *Proc. R. Soc. Lond.* A**384**, 381–401.

NOVIK, O. B. 1971 Model description of roll-waves. *J. Appl. Math. Mech.* **35**, 938–951.

ROACHE, P. J. 1976 *Computational Fluid Dynamics*. Hermosa.

WHITHAM, G. B. 1974 *Linear and Nonlinear Waves*. Wiley.